

# Battery-Integrated Modular Multilevel Converter Topologies for Automotive Applications

The background features several technical plots. At the top, there is a yellow waveform plot. Below it, a cyan waveform plot is visible. Further down, a red waveform plot is shown. A green sine wave is plotted in the middle section. At the bottom, there are orange and blue square-wave plots, and a final orange waveform plot. The plots are overlaid on a dark grid.

Arvind Balachandran



Linköping Studies in Science and Technology  
Licentiate thesis No. 1952

# Battery Integrated Modular Multilevel Converter Topologies for Automotive Applications

**Arvind Balachandran**



Division of Vehicular Systems  
Department of Electrical Engineering  
Linköping University  
SE-581 83 Linköping, Sweden

Linköping 2023

Linköping Studies in Science and Technology  
Licentiate thesis No. 1952

This is a Swedish Licentiate's Thesis.

Swedish postgraduate education leads to a Doctor's degree and/or Licentiate's degree.

A Doctor's degree comprises 240 ECTS credits (4 years of full-time studies).

A Licentiate's degree comprises 120 ECTS credits,  
of which at least 60 ECTS credits constitute a Licentiate's thesis.

Arvind Balachandran  
arvind.balachandran@liu.se  
www.vehicular.isy.liu.se  
Division of Vehicular Systems  
Department of Electrical Engineering  
Linköping University  
SE-581 83 Linköping, Sweden

**The cover:** The background photo shows the output waveform of a phase-shifted carrier-based modulation, including individual submodule voltages, the reference signal for the PLL, CAN bus communication signals, and a synchronization trigger signal.

Copyright © 2023 Arvind Balachandran unless otherwise noted.  
Published articles have been reprinted with permission from the respective copyright holder.

Balachandran, Arvind  
Battery Integrated Modular Multilevel Converter Topologies for Automotive Applications  
ISBN 978-91-8075-017-2 (PDF)  
ISBN 978-91-8075-016-5 (print)  
ISSN 0280-7971  
DOI <https://doi.org/10.3384/9789180750172>

Typeset using L<sup>A</sup>T<sub>E</sub>X 2<sub>ε</sub>  
Printed by LiU-Tryck, Linköping, Sweden 2023



This work is licensed under a Creative Commons Attribution 4.0 International License.

<https://creativecommons.org/licenses/by/4.0>

*"If you fail, never give up because FAIL means First Attempt In Learning."  
– A.P.J. Abdul Kalam*

*"All models are wrong, but some are useful."  
– George E. P. Box*



## Populärvetenskaplig sammanfattning

Behovet av hållbara transporter har lett till en snabb utveckling av elfordon, i dessa begränsar dock batteriet elfordonens körsträcka och livslängd. Ett batteri i ett fordon består av några tusen battericeller som vardera har spänningar runt 2-4 V och som är sammankopplade seriellt och parallellt i olika moduler och som gemensamt bidrar till batteriets spännings- och strömkapacitet. Variationer i tillverkningen av cellerna och andra faktorer gör att de individuella cellspänningarna och den procentuella laddningsfördelningen mellan cellerna kan variera under drift. Varje cell har en lägsta och högsta spänningsgräns som sätts och dessa gränser måste hållas för att batteriet inte skall förstöras. På grund av cell-till-cell variationerna når vissa celler gränserna snabbare än andra, vilket begränsar batteriets prestanda. En individuell cellstyrning är därför önskvärd för att maximera den energi som batteriet kan leverera.

Ett konventionellt framdrivningssystem för ett elfordon har ett batteri som levererar energi till en elektrisk maskin som används för framdrivning. Batteriet arbetar med likström medan elmaskinerna i fordon drivs med växelström, vilket gör att det behövs en kraftomvandlare som kan omvandla likströmmen från batteriet till växelström för elmaskinen. En sådan kraftelektronisk omvandlare som används för att omvandla likström till växelström, kallas för inverter och dessa använder i sin tur halvledarbrytare för att skapa växelströmmen. Uteffekten styrs genom att styra halvledarbrytarnas 'på'- och 'av'-period i invertern, så att utgången får en växelström. Hastigheten med vilken dessa övergångar växlar mellan 'på' och 'av' kallas för switchfrekvens. I en konventionell drivlina används vanligen en inverter som arbetar med två nivåer, därav namnet tvånivåomriktare, dessa har hög total harmonisk distorsion och kräver filter vid utgången (växelströmssidan). Total harmonisk distorsion är en avvikelse i vågformen från en ren sinusvåg. Ju högre den totala harmoniska distorsionen är, desto större är förlusterna i den elektriska maskinen.

För att minska dessa problem föreslås, presenteras och utvärderas batteriintegrerade modulära flernivåomvandlare (BI-MMC från engelskans Battery Integrated-Modular Multilevel Converter). I en BI-MMC kopplas mindre batterimoduler inom batteripaketet ihop med en inverter och blir då enheter som kallas submoduler. Liksom batterimoduler i ett konventionellt batteripaket kan dessa submoduler kopplas ihop seriellt och parallellt på ett sådant sätt att de kan leverera växelström direkt till den elektriska maskinen. En BI-MMC har därmed ökad styrbarhet och möjliggör en förbättring av batteripackets livslängd. Dessutom har en BI-MMC låg total harmonisk distorsion vid utgången, vilket ytterligare förbättrar drivlinans effektivitet.

Det första bidraget i avhandlingen handlar om att analysera och utvärdera olika topologier av tre- och sexfasiga BI-MMC:er. Som grund för jämförelsen används en konventionell tvånivåomriktare för ett 40-tons 400 kW lastbil. Utvärderingen visar att de flesta BI-MMC:er har lägre förluster än den konventionella tvånivåomriktaren. Det andra bidraget är en undersökning av hur antalet seriekopplade celler per submodul påverkar de totala förlusterna hos

en BI-MMC. Undersökningen visade att 5-6 seriekopplade celler per submodul har de lägsta förlusterna. Det tredje bidraget är konstruktionsprinciperna för optimering av submodulens filter på batterisidan och submodulens halvledaromkopplingsfrekvens, resultaten underbyggs också av en experimentell validering av förlustfördelningen inom en submodul.

Elektrokemisk impedansspektroskopi är en mätmetod som används för att karakterisera batteriers dynamiska prestanda och ger information om åldring och många andra egenskaper. Det fjärde bidraget är en metod för att bestämma batteriets elektrokemiska impedansspektrum med hjälp av omvandlarströmmen vid full belastning.

Laddningstiden för elfordon är betydligt längre än tankningstiden för konventionella fordon som drivs av flytande bränslen. För att få en kort laddningstid krävs effektiva likströmssnabbladdare, som kan leverera hög effekt. I ett konventionellt batterifordon kopplas batteriet direkt till snabbladdaren likströmsmatning, men i en BI-MMC är batteriet och invertern integrerade, vilket potentiellt ökar snabbladdningseffekten vid likströmsladdning eftersom spänningen kan vara högre under laddning än under drift. Det femte bidraget är därför en analys av och ett förslag på hur olika typer av BI-MMC topologier kan kopplas för att åstadkomma likströmssnabbladdning. Undersökningen visade att det är möjligt att utföra snabbladdning av en BI-MMC med likström och att det kan åstadkommas med försumbar inverkan på konstruktionen.



# Abstract

Electric vehicles are rapidly developing in response to the need for increasing sustainable energy sources. The range and lifetime of an electric vehicle are limited by the battery pack. A pack comprises modules with several parallel and/or series-connected cells. Differences in leakage currents and cell in-homogeneities cause individual cell voltage and state-of-charge distribution among the cells to be non-homogeneous. As a result, over time, some cells discharge faster than other cells, thus limiting the total energy delivered by the pack. In order to maximize the energy delivered by the pack, individual cell control is desirable. As a solution, battery-integrated modular multi-level converter (BI-MMC) topologies are proposed, presented, and evaluated. BI-MMC topology consists of either one or two arms per phase, and each arm comprises several cascaded stages of DC-AC converters and is commonly referred to as submodules. BI-MMCs provide increased controllability and potential improvement in the lifetime of the battery pack. Furthermore, BI-MMCs have low output total harmonic distortion, further improving the powertrain efficiency.

The first contribution is the design and evaluation of 3-phase and 6-phase BI-MMCs; comparisons are made against a conventional 2-level inverter for a 40-ton 400 kW commercial vehicle. The evaluation considers the total number of submodules, energy rating of the DC-link capacitors, battery losses, capacitor losses, and semiconductor losses. The evaluation showed that the BI-MMCs have lower semiconductor losses than the conventional 2-level inverter. However, the BI-MMCs have higher capacitor and battery losses. The second contribution is the investigation of the impact that the number of series connected cells per submodule has on the total losses of the BI-MMC. The study showed that 5- to 6-series connected cells have the lowest losses. The third contribution is the design principles for optimization of the DC-link capacitors and the MOSFET switching frequency; this is supported by experimental validation for the loss distribution within a submodule. The fourth contribution is a methodology for determining the battery impedance using the full-load converter current. In a conventional battery pack, the battery is connected directly to the fast charger's DC supply. However, in a BI-MMC, the battery and the inverter are integrated, potentially increasing the DC charging capabilities because higher voltages can be achieved during charging than during operation. The fifth contribution is thus the derivation and investigation of the maximum DC charging power of BI-MMCs assuming the same submodule semiconductor losses during traction. The analysis showed that most BI-MMCs have a maximum DC charging power of about 1 MW.



## Acknowledgments

Firstly, I would like to thank my supervisors, Tomas Jonsson and Lars Eriksson, for letting me start this unforgettable journey aboard the Ph.D. train. I thank them for being my co-authors, guiding me through research challenges, and making time for me despite their busy schedules. Tomas's extensive help in scientific reasoning and problem formulations and Lars's help with proofreading and guidance in scientific writing are very much appreciated. I want to thank the people at the Division of Vehicular Systems for providing an excellent working environment. Thank you, frequent fika room visitors, for exciting discussions during coffee breaks and for contributing to my listening comprehension of the Swedish language.

I want to thank all the people who helped me with my Swedish. Thanks to Christofer Sundström, Kristoffer Ekberg, Mattias Kryssander, and Oskar Lind Jonsson for letting me practice my Swedish communication skills with them. Lars Eriksson, Daniel Jung, and Tomas Jonsson are acknowledged for keeping me busy with teaching activities and helping me to develop my teaching skills. Thanks to Tobias Lindell for his support in the development of the laboratory.

Thanks to members of the Friday feast gang Theodor Westny, Jian Zhou, Arman Mohammadi, Shadi Hashemniya, Abhijeet Behera, Oskar Lind Jonsson, Arezou Safdari, and Ola Johansson for making weekly lunch sessions, after work activities, and a treasure hunt fun and memorable experiences. A special thanks to Oskar, the man with many names, for sharing the office and making our shared workspace a home away from home. Also, thanks to Theodor and Jian for sharing the office with me during the early days of my Ph.D. journey. Special thanks to Jian for accompanying me during the late-night sessions. Thank you Andrea for the study visit and showing me around Regensburg. Thanks to fellow members of the LiUPhD board for the fruitful discussions about life as a Ph.D. student, broader research perspectives, and co-organizing Nobel dinners.

Thanks to all my friends for not forgetting me and listening to me nag about my research. I had fun whenever we traveled together, visited you, or when you visited me, it's always fun. I would also like to thank my parents for supporting and believing in me. Thank you very much for that!

Linköping, January 2023



Arvind Balachandran

## Funding

This work was supported by stiftelsen för miljöstrategisk forskning (Mistra) and in collaboration with Scania CV, Chlamers and Svenska Elektromagneter AB.



---

# Contents

<b>1</b>	<b>Introduction</b>	<b>1</b>
1.1	Battery Technologies: A Brief History . . . . .	2
1.2	Electric Vehicle Classification . . . . .	3
1.3	Conventional Battery Electric Vehicle Powertrain . . . . .	3
<b>2</b>	<b>Background</b>	<b>5</b>
2.1	Reconfigurable Battery Systems . . . . .	5
2.2	Battery-Integrated Modular Multilevel Converters . . . . .	7
<b>3</b>	<b>Thesis Focus and Contributions</b>	<b>13</b>
3.1	List of Publications . . . . .	15
3.2	Future Work . . . . .	20
	<b>References</b>	<b>21</b>
	<b>Papers</b>	<b>29</b>
<b>I</b>	<b>Design and Analysis of Battery-Integrated Modular Multi-level Converters for Automotive Powertrain Applications</b>	<b>31</b>
1	Introduction . . . . .	32
2	Topology review . . . . .	33
3	BI-MMC: Modeling and Design . . . . .	34
4	Comparative Assessment . . . . .	40
5	Discussion . . . . .	44
6	Conclusion . . . . .	44
	References . . . . .	45

<b>II</b>	<b>Experimental Evaluation of Battery Impedance and Submodule Loss Distribution for Battery Integrated Modular Multilevel Converters</b>	<b>49</b>
1	Introduction . . . . .	50
2	Topology overview . . . . .	51
3	Loss-distribution . . . . .	52
4	Experimental determination of impedances and losses . . . . .	54
5	Conclusion . . . . .	59
	References . . . . .	60
<b>III</b>	<b>An Overview of 3- and 6-phase Battery Integrated Modular Multilevel Converters for Automotive Applications</b>	<b>63</b>
1	Introduction . . . . .	64
2	Topology Review . . . . .	66
3	Modeling and Design . . . . .	74
4	Design Parameters . . . . .	80
5	Comparative Assessment . . . . .	82
6	Performance Matrix . . . . .	88
7	Conclusion . . . . .	89
	References . . . . .	91
<b>IV</b>	<b>DC Charging Capabilities of Battery-Integrated Modular Multilevel Converters Designed Based on a Maximum Tractive-Power</b>	<b>97</b>
1	Introduction . . . . .	98
2	Topology Review . . . . .	99
3	Total Number of Submodules . . . . .	101
4	Power Loss Calculations . . . . .	102
5	Maximum DC Charging Power Calculations . . . . .	104
6	Submodule Case Temperature . . . . .	105
7	Comparative Assessment . . . . .	105
8	Discussion . . . . .	111
9	Conclusion . . . . .	112
	References . . . . .	113

# 1

---

## Introduction

Transportation is crucial in society and plays a vital role in economic growth [1]. Road freight transportation is the backbone of trade and commerce in the European Continent, and heavy-duty vehicles (HDVs) carry about 71.3% of the freight transport over land [2]. Moreover, about 98% of the HDV fleet is powered by diesel [2], contributing to about 25% of the EU automotive greenhouse-gas emissions [3]. The automotive industry accounts for about 15% of CO<sub>2</sub> emissions worldwide and about 20% in the EU [4, 5]. The global CO<sub>2</sub> emissions from fossil fuels in the transportation sector have increased from about 5.18 GtCO<sub>2</sub> in 2010 to about 6 GtCO<sub>2</sub> in 2022 [6–8]. These increased greenhouse gas emissions have led to a considerable increase in the average global temperature over the last few decades [9].

As part of the global effort to limit global warming, intergovernmental organizations, such as the European Commission, have introduced stricter legislation standards to ensure zero-emission mobility within the next few years [10]. Furthermore, recent battery technology advancements have made it possible to have cheaper electric vehicles (EV) with longer driving ranges [11]. These factors have led to the rapid development of EVs. However, despite these valiant efforts, only Sweden, China, and Norway have, on average, more than 1% of EV share [12]. Electric HDVs only hold about 0.1% of the HDV market share, but these numbers are expected to proliferate [13]. Several leading HDV manufacturers such as Volvo, Scania, Mercedes-Benz, MAN, DAF, and IVECO have announced plans to transition to 100% electric HDV sales by 2040 [13].

[14] describes *range anxiety* as the EV driver’s fear of running out of electricity before reaching another available charging station. This is one of the most crucial

factors influencing purchasing an EV or conventional internal combustion engine (ICE) vehicle [12, 15]. In addition to *range anxiety*, the lifetime is also crucial for HDVs because they have higher mileage than passenger cars. For example, in Sweden, HDVs have a mileage of over 55,000 km annually, nearly five times the annual mileage of a typical passenger car [16]. To alleviate *range anxiety* and increase the lifetime of EVs, battery integrated-modular multilevel converter (BI-MMC) topologies are proposed, presented, and evaluated in this thesis.

The thesis outline follows: Chapter 2 presents the state-of-the-art solutions to increase the range and lifetime of EVs, and Chapter 3 presents the contributions and the thesis outlook.

The outline of this chapter follows: Section 1.1 presents a brief history of battery technologies, Section 1.2 presents different EV classifications, and Section 1.3 presents the conventional battery-based EV powertrain and the challenges concerning them.

## 1.1 Battery Technologies: A Brief History

Batteries (or electrochemical cells) are electrochemical devices that convert chemical energy into electrical energy. There are three basic components in a battery, they are the positive electrode, the negative electrode, and the electrolyte [17]. During discharge, The positive electrode accepts the electrons from the electric circuit, the negative electrode emits electrons to the circuit, and the electrolyte provides a path for ions to flow between the positive and negative electrodes inside the battery [17, 18]. During charging, the roles of the positive and negative electrodes are reversed.

There is some belief that the first electrochemical battery, called the 'Baghdad Battery', existed as old as the first century BC [19]. However, the closest resemblance to today's batteries, the zinc-carbon battery, was developed in 1866 by Georges-Lionel Leclanché [20]. The zinc-carbon battery is a non-rechargeable (primary) battery that is designed for one-time use and today, these batteries have found their applications in flashlights, computer keyboards, etc. For applications that require more energy such as automobiles, laptops, etc. rechargeable (secondary) batteries are preferred. In 1859, Gaston Planté invented lead-acid, and in 1901, Waldmar Jungner discovered the nickel-cadmium rechargeable batteries [19]. Today, these batteries can be found in power supplies for car ignition and portable tools.

The demand for high energy and high power sources with high energy density had increased significantly in the 1960s [21]. The low energy densities of lead-acid and nickel-cadmium batteries were a major drawback, and these batteries were too heavy to satisfactorily serve the evolving technology. The breakthrough came with the discovery of the Lithium-ion battery with an energy density of about four to five times that of lead-acid and nickel-cadmium batteries [19, 21]. Furthermore, Lithium-ion batteries have an improved operation lifespan than lead-acid and nickel-cadmium batteries [19, 21]. Today, Lithium-ion batteries,



due to their high-energy efficiency, are ideal candidates for EVs [22].

## 1.2 Electric Vehicle Classification

Electric vehicles (EV) are broadly classified, based on their powertrains, in four different ways, they are as follows [23]:

1. Plug-in hybrid electric vehicles (PHEV)
2. Hybrid electric vehicles (HEV)
3. Fuel-cell-based electric vehicles (FCEV), and
4. Battery electric vehicles (BEV).

PHEVs and HEVs incorporate a battery pack, a traction motor, and an internal combustion engine for propulsion. PHEVs primarily use a battery pack and traction motor for propulsion and are supported by a small internal combustion engine for longer driving ranges. However, HEVs primarily use an internal combustion engine for propulsion and are supported by a traction motor, powered by a small battery pack, to improve the powertrain efficiency. Furthermore, the battery pack in PHEVs can be recharged from an external power source, whereas the HEV battery pack cannot be recharged from an external power source.

Unlike PHEVs and HEVs, FCEVs and BEVs are all-electric vehicles and are commonly called EVs, i.e., they do not incorporate an internal combustion engine for propulsion. An FCEV powertrain contains fuel cells that use electrochemical processes to convert fuels, such as hydrogen, into electricity, which is used to power a traction motor. Although the primary energy carrier in an FCEV is the hydrogen fuel cell, a battery pack is required to ensure smooth power to/from the fuel cell. BEVs have a large battery pack, and the electrical energy from the pack is directly used to power the traction motor, which propels the vehicle. The battery pack in BEVs needs to be recharged from an external power source.

## 1.3 Conventional Battery Electric Vehicle Powertrain

The energy stored in the battery pack of an EV is analogous to the 'fuel tank' in a conventional internal combustion engine-based vehicle. All electric vehicles (BEVs, in particular) employ battery packs that require high energy and power [24]. High power implies a high current and voltage, but high currents result in increased power losses and, thus, lower powertrain efficiency. Therefore, it is preferred to have a high voltage than a high current. Lithium-ion batteries (or Lithium-ion cells), due to their high-energy efficiency, are ideal candidates for electric vehicles [22], but Li-ion cells typically have very low output voltages somewhere between 2-4 V [25]. Furthermore, Li-ion cell construction places limits on cell current [25]. The power required by the EV is far greater than the power a

single Li-ion cell can deliver. To mitigate this problem, an electric vehicle battery pack typically consists of a combination of cells interconnected in both series and parallel. EV battery packs typically have a voltage of 300-800 V [26], which defines the number of series-connected cells. The battery pack's voltage and energy determine the pack's capacity, defining the number of parallel-connected cells. A battery pack in an electric vehicle consists of a few thousand hard-wired series- and parallel-connected battery cells. For instance, a Tesla Model 3 consists of about 4000 cells, and a commercial truck can have around 5000 cells with total energy exceeding 500 kWh [27, 28]. Due to variations in the manufacturing of the cells and several other factors, the distribution of voltages and the state-of-charge among the cells are non-homogeneous and vary during operation [29]. Furthermore, each cell has a set minimum and maximum voltage limit, and these limits must be maintained to prevent the battery from being destroyed [30]. As a result, the range and lifetime of BEVs are limited by the battery pack, in particular, the weakest cell of the pack.

Figure 1 presents a block diagram of a conventional BEV powertrain. The figure shows the large battery pack with hard-wired series and parallel cells that supply the energy to a traction motor for propulsion. The battery pack consists of several strings of series-connected cells, along the  $y$ -axis, and parallel-connected cells, along the  $x$  and  $z$  axes. The strings with weak cells, highlighted in red, limit the battery pack's output power, and over time, these weak cells significantly limit the total energy available from the pack. Therefore, individual cell control is preferred to maximize the energy the battery pack can deliver. The figure also shows a power converter that converts the direct current (DC) from the battery to a regulated alternating current (AC) to the traction motor. Such a power electronic converter is called an inverter.

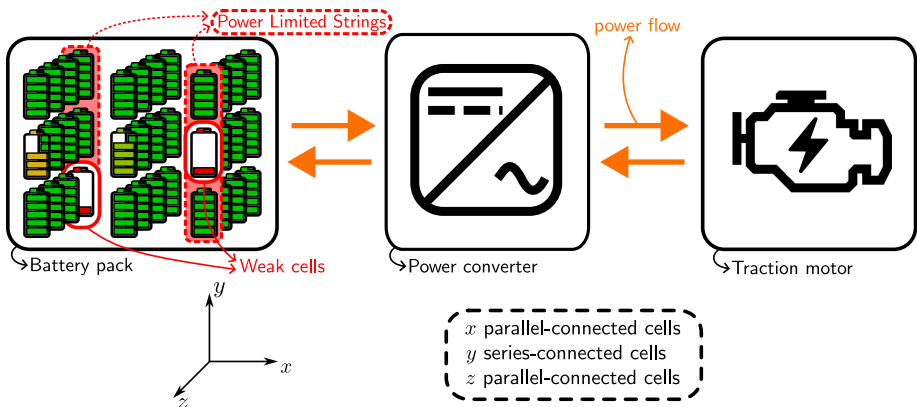


**Figure 1:** Conventional battery electric vehicle powertrain.

# 2

---

## Background

As presented in Chapter 1, individual cell control is preferred to maximize the energy the battery pack can deliver. Increasing individual cell control is often achieved by reconfiguring battery cells by integrating power electronics into the battery pack. This can change the battery interconnection pattern in response to the battery behavior and user demands. Furthermore, this provides enhanced fault tolerance, charge and temperature balancing, extended energy delivery, and easy integration of batteries of different ages and chemistries [31]. Although there are several benefits to integrating power electronics in battery packs, critical challenges, such as advanced power electronic switching topologies, complex control algorithms, and complex optimization algorithms, must be addressed. Several complex optimization and control algorithms are developed and presented in [32–35].

The state-of-the-art research in integrating power electronic switching topologies can be broadly classified into two: reconfigurable battery systems, which is presented in Section 2.1 and battery-integrated modular multilevel converters, which is given in Section 2.2.

### 2.1 Reconfigurable Battery Systems

Figure 1 shows the block diagram of a reconfigurable battery pack (RBP) based BEV powertrain. It is similar, in structure, to the conventional powertrain but power electronics are integrated into the battery pack. RBPs use semiconductor switches, such as MOSFETs, to disconnect and connect individual battery cells.

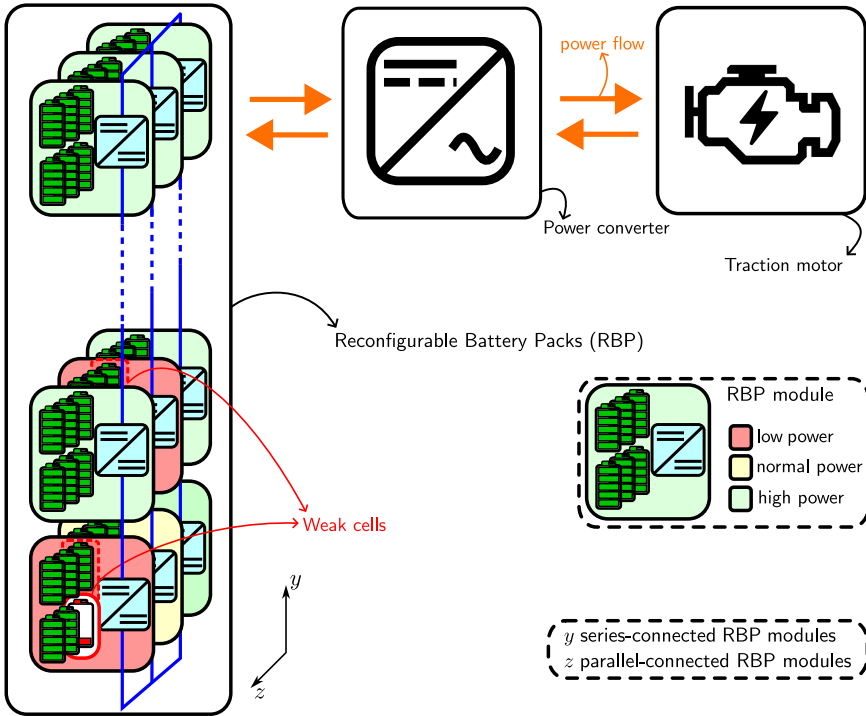


**Figure 1:** Reconfigurable battery pack-based battery electric vehicle powertrain.

In the figure, these MOSFET switch combinations (topologies) are represented as DC-DC converters (blue blocks) and are called RBP modules. The two coordinates ( $y$  and  $z$ ) show the interconnection of RBP modules. The total DC-link voltage of the system determines the number of series-connected RBP modules along the  $y$ -axis, and the total energy of the battery back determines the total number of parallel-connected RBP modules along the  $z$ -axis. The RBP modules can be classified based on the number of switches per module: Subsections 2.1.1 and 2.1.2 describe the RBP modules with two and three switches, respectively.

### 2.1.1 Reconfigurable Battery Pack Module with 2 switches

Figure 2 shows the basic schematic of different RBP modules. The most straightforward RBP module design includes two switches (2-switch RBP module) is shown in Figure 2(a). One switch is used to connect (insertion state) and the other is used to disconnect (bypass state) the cell from the RBP. This design has several advantages when compared to the conventional powertrain, such as simple hardware design, enhanced fault tolerance and safety, improved energy efficiency, balanced system operation, increased charge delivery, longer operating times, and customizable terminal voltages [36–39].

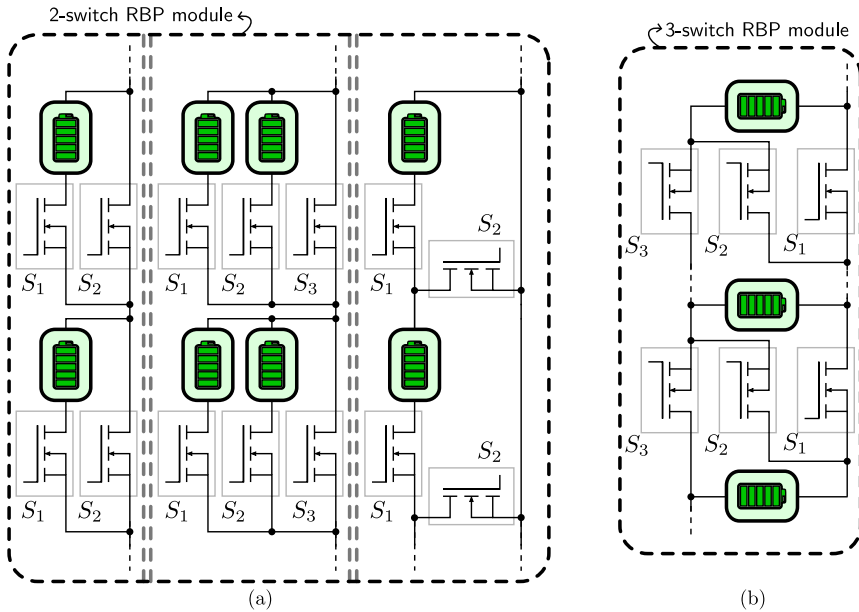


**Figure 2:** Reconfigurable battery pack modules with 2 and 3 switches per module.

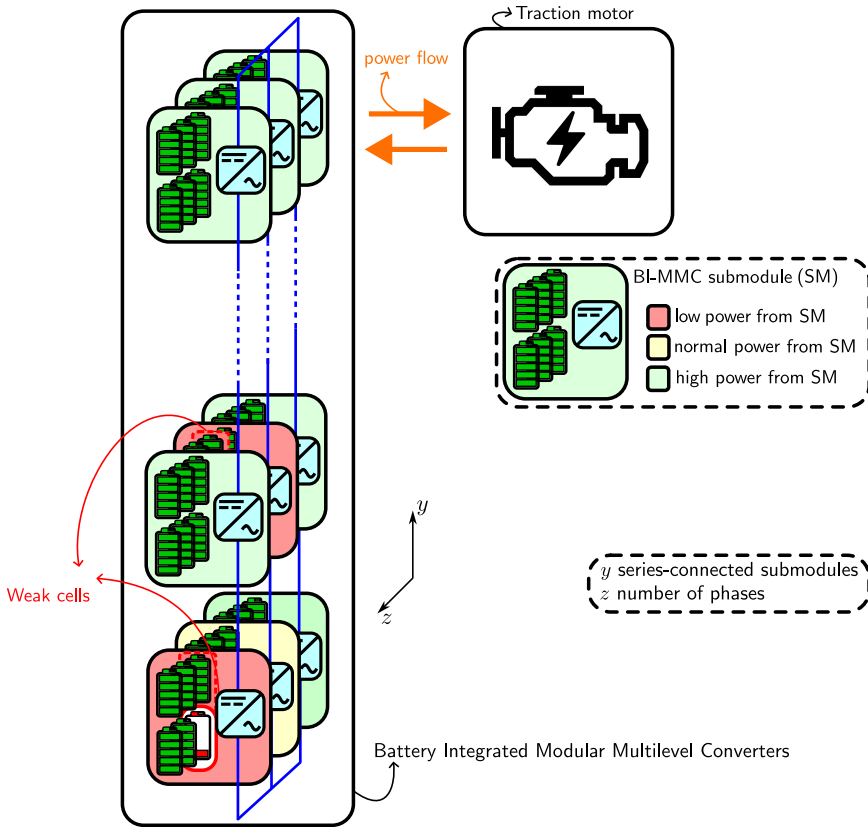
### 2.1.2 Reconfigurable Battery Pack Module with 3 switches

Figure 2(b) shows an RBP module topology with three switches (3 switch RBP module). This enables parallel connection of several modules and provides a prolonged battery life span [40–42]. More complex RBP module designs with four or more switches further increase the controllability and lifetime of the battery pack [43–46].

RBPs are simple in design and easy to integrate into existing conventional BEV powertrains. However, they still incorporate a 3-phase two-level inverter. Although simple in design and control, two-level inverters often require large filters at the AC side (output side) to achieve good electromagnetic compatibility [47]. In order to further improve powertrain efficiency, battery-integrated modular multilevel converters are developed.

## 2.2 Battery-Integrated Modular Multilevel Converters

Figure 3 shows the block diagram of battery-integrated modular multilevel converter (BI-MMC) based BEV powertrains. In BI-MMC powertrains, the inverter is integrated into the battery pack, thus minimizing the number of power conversion stages and increasing the total powertrain efficiency [48]. Furthermore, a multilevel output voltage (traction motor voltage) can be achieved with BI-



**Figure 3:** Battery-integrated modular multilevel converter based battery electric vehicle powertrain.

MMCs as opposed to 2-levels from the conventional powertrain [47]. This reduces the size of the output AC filter and losses in the traction motor, further improving the powertrain efficiency [49].

The section outline follows: Subsection 2.2.1 presents, in brief, a background on modular multilevel converters. Subsections 2.2.2 and 2.2.3 present the half- and full-bridge BI-MMC submodules, respectively. Subsection 2.2.4 presents modular multilevel series-parallel converters, and battery modular multilevel management converters are presented in Subsection 2.2.5.

### 2.2.1 Modular Multilevel Converters

Modular multilevel converters (MMCs) have gained popularity, especially in high voltage (HV) power grid applications where its proven to have several advantages such as low total harmonic distortion (THD), high modularity, and improved scalability [50]. THD can be defined as a distortion of the waveform from a pure

sine wave with a specific fundamental frequency. Lower THD implies lower ripple currents, reduction of bulky filters on the AC side, and higher traction motor efficiency [51]. MMCs typically have one or two arms per phase, and each arm includes several cascaded stages of DC-AC converters, commonly referred to as submodules (SM) (also referred to as cells or chain links). MMC SMs typically incorporate a capacitor, and as long as the capacitor voltage is constant, the SMs behave as controllable voltage sources.

The key difference between an MMC and a BI-MMC is the SM design. In BI-MMCs, the SMs incorporate a battery module with  $N_s(\text{cells})$  series- and  $N_p(\text{cells})$  parallel-connected cells (Figures 4 to 6) while MMCs use capacitors. In Figure 3, the two coordinates ( $y$  and  $z$ ) show the interconnections between BI-MMC SMs. The maximum peak voltage of the traction motor determines the number of series-connected SMs along the  $y$ -axis, and along the  $z$ -axis is the number of phases.

Over the last few years, BI-MMCs have gained popularity in research and development, especially for second-life battery applications such as power-grid stabilization [52–54]. BI-MMCs are particularly interesting for EV powertrains since it has high efficiency and provides greater cell-level control [55, 56]. BI-MMCs can improve battery balancing and provide better battery fault isolation due to their highly modular structure [57].

## 2.2.2 Half-Bridge Submodules

Figure 4 presents the schematic of two BI-MMC SMs. Figure 4(a) shows the most straightforward SM design, the half-bridge submodule (HB-SM), with two switches. Similar to 2-switch RBP modules, HB-SMs also have two output states, i.e., insertion and bypass states. The design and control of HB-SM-based BI-

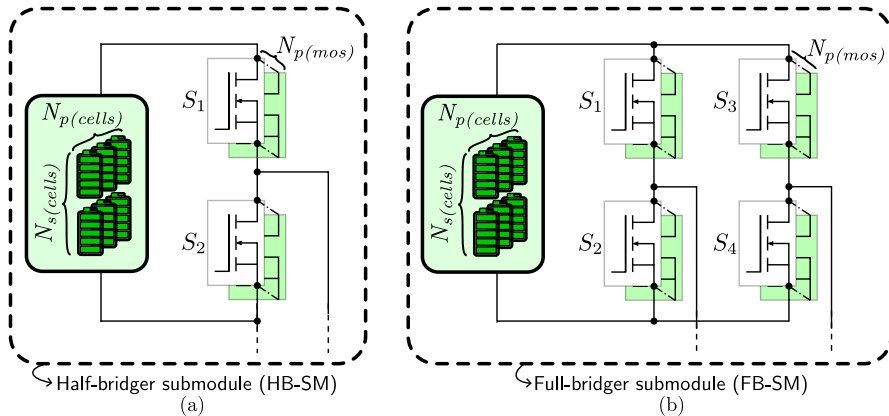


**Figure 4:** Battery-integrated modular multilevel converter submodules. (a) half-bridge submodule and (b) full-bridge submodule.

MMC with active balancing strategies were presented in [58, 59]. It was found that HB-SM-based BI-MMCs, actively equalize the cells, thus improving the performance of the battery pack. Furthermore, they have many output voltage levels that strongly reduce the THD of motor voltages, thus reducing traction motor power losses. HB-based MMCs also have increased fault-ride-through capabilities of EV battery packs, increasing the longevity of EV battery packs [60, 61].

### 2.2.3 Full-Bridge Submodules

The full-bridge submodules (FB-SM) with four switches are shown in Figure 4(b). Unlike the HB-SM, in the FB-SM two insertion states are possible: a positive insertion state occurs when the SM's output voltage is positive, and a negative insertion state occurs when the output voltage of the SM is negative. The FB-SM is thus known to have a bipolar output voltage, thereby improving the power density when compared to HB-SMs [62]. Furthermore, the FB-SM battery current contains fewer harmonics than the HB-SM, and as a result, FB-SM-based BI-MMCs have a higher converter efficiency than HB-SM-based BI-MMCs [63]. The FB-SM-based BI-MMC with one arm per phase are widely used and are called cascaded H-bridge inverters (CHB) [64]. Compared to a conventional EV powertrain with a 2-level inverter using IGBTs, CHBs have improved efficiency and easier expandability from 400 to 800 V systems [63, 65].

### 2.2.4 Modular Multilevel Series-Parallel Converters

A significant challenge with the HB- and FB-SM designs are the high harmonic content of the battery current, thereby increasing the battery losses [63]. Therefore, modular multilevel series-parallel (MMSP) converters were developed to reduce battery losses [66], and an MMSP-SM is shown in Figure 5. [67] presents a comparative assessment of MMSP, CHB, and the conventional two-level inverter. The analysis shows that MMSP inverters have higher efficiencies than

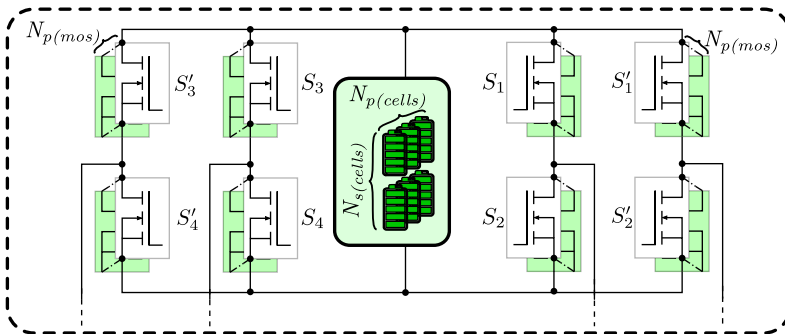


**Figure 5:** Modular multilevel series-parallel converter submodule.



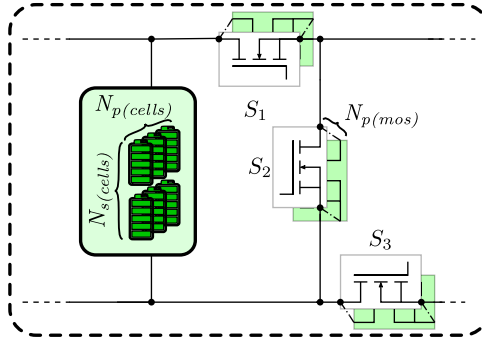


**Figure 6:** Battery modular multilevel management (BM3) converter submodule.

the two-level inverter at both partial and peak loading. Furthermore, MMSPs showed higher efficiency than the CHBs.

### 2.2.5 Battery Modular Multilevel Management Converters

Figure 6 presents a battery modular multilevel management (BM3) converter SM. In a BM3 SM, the switches can connect battery modules in series or parallel, depending on the desired voltage level. The BM3 systems were first introduced in [68], and when compared to the CHB inverters, BM3s reduce the number of switches for the same output voltage levels [69]. However, when compared to MMSP, BM3 inverters have higher losses [70]. Performance analysis of BM3 inverters was presented in [71], and it was concluded that increasing the number of cells per submodule increases the overall efficiency.

Thus far, the analysis considers BI-MMC operation during traction with partially or fully charged battery packs. The additional advantage of BI-MMCs is that the requirement of an onboard charger (OBC), necessary for AC charging of conventional EVs, becomes obsolete. [72, 73] showed that BI-MMCs could operate in grid-tied mode to charge the individual battery packs. Furthermore, [74, 75] reported several advantages with BI-MMCs while charging, such as active balancing during charging and providing a flexible DC charging voltage.



# 3

---

## Thesis Focus and Contributions

The main focus of the thesis is the evaluation of multi-phase battery-integrated modular multilevel converter (BI-MMC) topologies for a 400 kW 40-ton heavy-duty vehicle. The evaluation includes five different topologies considering both half- and full-bridge submodules under three main systems: 3-phase, 6-phase low-voltage, and 6-phase high-voltage. The topologies are namely: double-star half-bridge (DSHB), double-star full-bridge (DSFB), single-star half-bridge (SSHB), single-star full-bridge (SSFB, or cascaded H-bridge), and single-delta full-bridge (SDFB). The effect of the number of cascaded cells per submodule for all BI-MMCs on the total power losses and the maximum DC charging power is investigated. A three-phase 2-level SiC MOSFET-based inverter is considered the reference case for the topology evaluation.

An interactive Matlab application called the *topology evaluation dashboard* was developed and is shown in Figure 1. In the dashboard, the user can input different parameters, such as average and maximum power during traction, MOSFET on-state resistance, thermal resistances, battery cell nominal voltage, battery cell capacity, stray inductances, etc. The user can also select and compare different topologies, systems, and the number of cascaded cells per submodule. The evaluation results are saved as a `.mat` file or visualized directly as plots in the various tabs, as shown in Figure 1. The intended use of the dashboard is to provide the engineer with a tool for investigating the effect of the number of cascaded cells, topologies, systems, design parameters, assumptions, and constraints on the losses and cost of multi-phase BI-MMC topologies.

A performance matrix for all the BI-MMC topologies under the three main systems with 1 to 12 cascaded cells per submodule is presented in Paper III

Selection of Topologies, number of cascaded cells per submodule and systems evaluation results

The screenshot shows the Matlab application interface for evaluating battery-integrated modular multilevel converter topologies. The interface is organized into several main sections:

- Topologies:** A list of converter topologies including DSB8, SSB8, SSB9, and SSB9B. The 'Number of cells' for each is specified (e.g., 11 for DSB8, 9 for SSB8).
- Converter Parameters:** Fields for 'Average output power [W]' (1400), 'Rated output voltage [V]' (440), 'Maximum modulation index' (0.83), 'Incl. power factor' (0.9), and 'Submodule pulse number' (6).
- Battery Parameters:** Fields for 'Minimum battery cell voltage [V]' (3.25), 'Normal cell voltage [V]' (3.7), 'Maximum cell voltage [V]' (4), 'Energy of battery pack [Wh]' (14096), 'Depth of discharge' (0.65), and 'Normal cell capacity [Ah]' (28).
- Thermal Parameters:** Fields for 'Maximum ambient temperature [degC]' (40), 'Case to ambient heat transfer coefficient [W/m^2K]' (400), 'MOSFET case [m^2]' (0.004), and 'Heat transfer area [m^2]' (0.008).
- Cost Constants:** Fields for 'Cost per submodule [€/\$]' (50), 'Capacitor cost per unit [€/\$]' (1), 'Cost per kWh [€/\$/kWh]' (120), and 'MOSFET cost [€/\$]' (3.3 3.3 3.3 3.3 3.3).
- MOSFET switching parameters:** Fields for 'Rise-time fall [μs]' (500), 'Fall-time fall [μs]' (500), 'Rise-time fall [μs]' (2000), 'Fall-time fall [μs]' (2000), 'Submodule DC voltage reference [V]' (50), and 'PCU gate-time inductance [H]' (2e-6).
- Motor and drive-cycle parameters:** Fields for 'Number of poles of motor' (20), 'Motor Nominal speed [rpm]' (1000), 'DC charging voltage [V]' (7250), 'DC charging current [A]' (3000), 'DC charging voltage [V]' (7250), and 'DC charging average submodule dir. cycle [h]' (85).
- DC Charging:** Checkboxes for 'DC charging enable', 'MOSFET loss for DC charging voltage', and 'Override Optimization'.
- Battery modeling:** Checkboxes for 'Enable pulsed charging' and 'Include Cap Loss in DCC'. A 'DC impedance frequency [Hz]' field is set to 1.
- Capacitor modeling:** Fields for 'Peak DC-link current for 1 series-cells per submodule [A]' (5), 'Maximum energy for 1 series-cells per submodule [J]' (0.088), 'Maximum energy for a submodule capacitor [J]' (0.03), 'Maximum power dissipation for a submodule capacitor [W]' (0.23), 'DC-link capacitor DF 2-level [μs]' (1.93), 'DC-link capacitor ECL [H]' (6e-8), 'DC-link capacitor ECL [H]' (0.01), and 'Total energy stored in SCL & link capacitor [J]' (350).
- 2-level inverter:** Fields for 'DC-link voltage [V]' (800), '2-level inverter pulse number' (60), 'DC-link capacitor energy 2-level [J]' (992), 'DC-link capacitor DF 2-level [μs]' (1.93), 'DC-link capacitor ECL [H]' (6e-8), 'Thermal resistance case to ambient [K/W]' (0.01), and 'Battery Lead inductance 2-level [H]' (1e-7).
- MOSFET selection:** Radio buttons for 'MOSFET - Vahdipad CAB-00412XG3 - SIC', 'MOSFET - SEMIKRON SKM300B100GCH17 - SIC', and 'MOSFET - IXYS IXM300P120T5F - Si-Bridge'.
- Optimization options:** Checkboxes for 'Optimizing minimum number of parallel MOSFETs', 'Battery loss reduction factor [x]' (3), 'Optimized pulse number and capacitor energy', and 'Capacitor under-rating factor [x]' (10).
- Information:** A note stating 'Battery you can use the application, Battery model and gate driver are created using MATLAB'.
- Run:** A 'Run' button with a status indicator showing 'Completed'.

Figure 1: Battery integrated modular multilevel converter evaluation dashboard Matlab application screenshot.

and an interactive version is available in gitlab<sup>1</sup>. The performance matrix aids the user to perform a cost-benefit comparative assessment of all the BI-MMC topologies.

## 3.1 List of Publications

The Main contributions of the individual papers are summarized in this section. The author contributed most of the research, presentation, and analysis.

Paper I presents the design principle for 3-phase BI-MMC topologies for a 40-ton 400 kW heavy-duty vehicle. The design principle is validated in Paper II. Paper III extends the design principle in Paper I to 6-phase BI-MMC topologies. The articles above consider BI-MMC design for maximum traction power of 400 kW with partially or fully charged battery packs. Paper IV thus presents the DC charging capabilities of BI-MMCs assuming similar submodule semiconductor losses as in Paper I.

### **Paper I: Design and Analysis of Battery-Integrated Modular Multilevel Converters for Automotive Powertrain Applications**

by Arvind Balachandran, Tomas Jonsson, and Lars Eriksson. *23rd European Conference on Power Electronics and Applications (EPE'21 ECCE Europe)*, 978-9-0758-1537-5, 2021.

The design principle for a wide range of 3-phase BI-MMC topologies is developed. The design principle is based on the loss distribution between the battery and the DC-link capacitors in a submodule. The loss distribution is driven by the energy stored in the submodule DC-link capacitors and MOSFET switching frequency. Therefore an optimization problem is formulated to minimize the total losses at rated power and determine the optimal energy stored in the submodule DC-link capacitors and MOSFET switching frequency. The optimization is implemented on five different 3-phase BI-MMC topologies each with 1 to 12 cascaded cells per submodule.

A comparative assessment of the aforementioned BI-MMC topologies considering 1 to 12 cascaded cells per submodule is performed. Furthermore, the comparative assessment considers a 3-phase 2-level SiC MOSFET-based voltage source converter as the reference case. The comparative assessment includes the total number of submodules, battery, capacitor, and semiconductor losses. The intended use of the assessment is to aid the engineer in selecting the optimal DC-link capacitor size, switching frequency, and the number of cascaded cells per submodule for a given design requirement. Although the assessment is performed for an automotive application, the procedure is generic and can be extended to battery energy storage systems.

---

<sup>1</sup>[https://gitlab.liu.se/BI-MMC\\_public/the\\_performance\\_matrix](https://gitlab.liu.se/BI-MMC_public/the_performance_matrix)

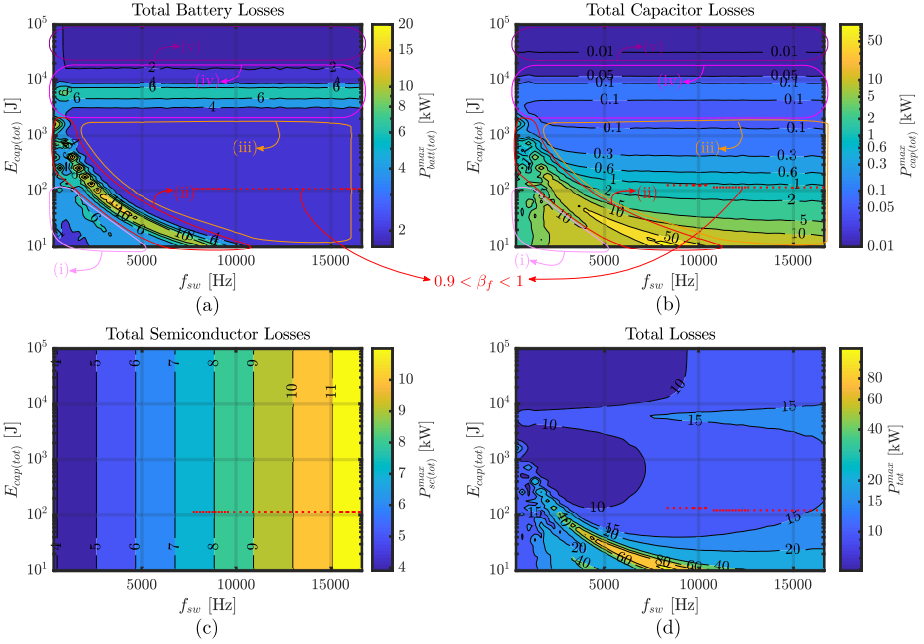


**Figure 2:** Power losses as a function of the total energy stored in the DC-link capacitors in a submodule ( $E_{cap(tot)}$ ), and the MOSFET switching frequency ( $f_{sw}$ ) for 3-phase 5 cascaded cells per submodule ( $N_{s(cells)}$ ) double-star full-bridge (DSFB) BI-MMC topology at a rated power of 400 kW presented in Papers I and II. (a) total battery losses ( $P_{batt(tot)}^{max}$ ), (b) total capacitor losses ( $P_{cap(tot)}^{max}$ ), (c) total semiconductor losses ( $P_{sc(tot)}^{max}$ ), and (d) total converter losses ( $P_{tot}^{max} = P_{batt(tot)}^{max} + P_{cap(tot)}^{max} + P_{sc(tot)}^{max}$ ). Furthermore, (a) and (b) shows submodule loss distribution regions related to  $f_{sw}$  and resonance ( $f_{res}$ ) between the battery and DC-link capacitors in a submodule. Region (i):  $f_{sw} < f_{res}$ , region (ii):  $f_{sw} \approx f_{res}$ , region (iii):  $f_{sw} > f_{res}$ , region (iv):  $f_{sw} \approx 2f_1$  ( $f_1$  is the output current/voltage fundamental frequency), and region (v):  $f_{sw} > 2f_1$ .

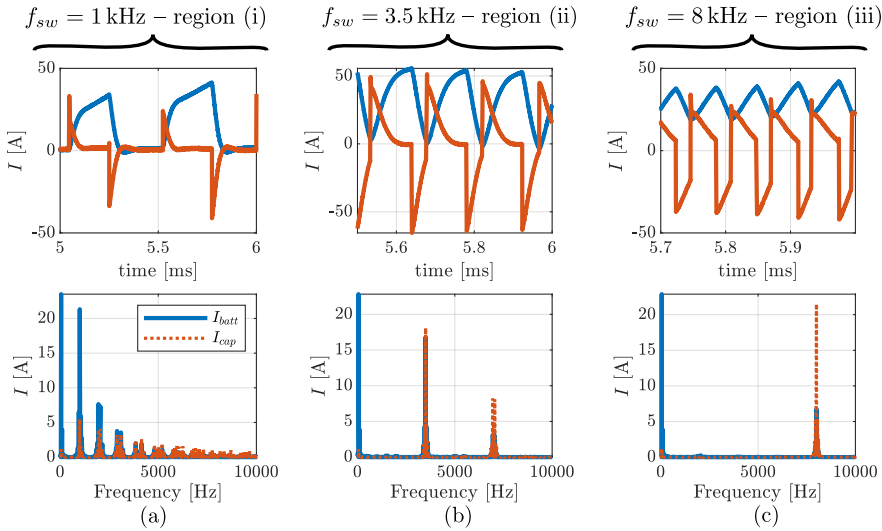


**Figure 3:** Measured battery- and calculated capacitor-currents at different converter switching frequencies ( $f_{sw}$ ) presented in Paper II. The allocation of harmonics at different regions between the battery and the DC-link capacitors in a submodule is shown. (a) battery and capacitor current time plot and frequency spectra with  $f_{sw} = 1$  kHz, in the region (i), (b)  $f_{sw} = 3.5$  kHz, in the region (ii), and (c)  $f_{sw} = 8$  kHz, in the region (iii).

The evaluation showed that all the 3-phase BI-MMCs have lower semiconductor losses than the conventional 2-level inverter. However, the capacitor and battery losses for the BI-MMCs are significantly higher. Furthermore, the study shows that full-bridge SM-based BI-MMCs with 5 to 6 cascaded cells per submodule have lower total converter losses than the 2-level inverter.

## Paper II: Experimental Evaluation of Battery Impedance and Submodule Loss Distribution for Battery Integrated Modular Multilevel Converters

by Arvind Balachandran, Tomas Jonsson, Lars Eriksson, and Anders Larsson. *24th European Conference on Power Electronics and Applications (EPE'22 ECCE Europe)*, 978-9-0758-1539-9, 2022.

The DC-current harmonics allocation and, in turn, the loss distribution between the battery and the DC-link capacitors in a submodule, presented in Paper I, is experimentally validated. The experiments are performed on a single-phase half-bridge converter, the battery and the submodule DC-side currents are measured, and the losses are determined at different MOSFET switching frequencies. Furthermore, a methodology to characterize the battery impedance utilizing the full-load converter switching currents (switched pulse test) is presented.

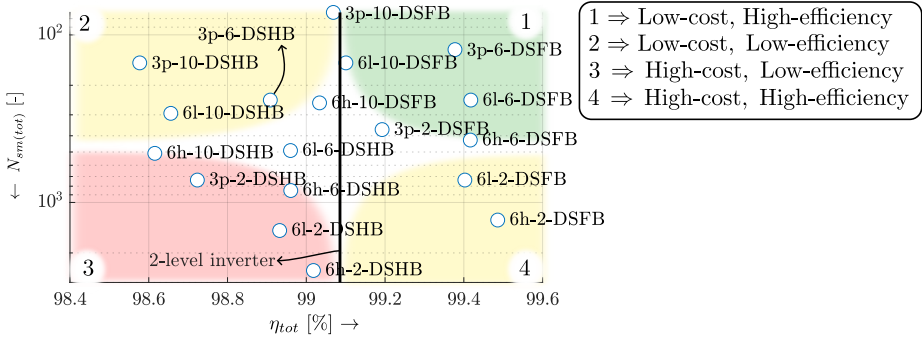


**Figure 4:** The performance matrix, the total number of submodules ( $N_{sm(tot)}$ ) vs. efficiency ( $\eta_{tot}$ ) during traction, for all BI-MMC topologies with 2, 6, and 10 cascaded cells per submodules ( $N_{s(cells)}$ ) at an average power of 100 kW presented in Paper III. The four quadrants of the x-y plane depict four performance measures: the first quadrant (green) represents topologies with low-cost and high efficiency, the second quadrant (yellow) indicates low-cost and low efficiency, and the third quadrant (red) and the fourth quadrant indicates high-cost low-efficiency, and high-cost high-efficiency, respectively. Furthermore, the performance matrix follows the nomenclature, 'ph- $N_{s(cells)}$ -Top,' where ph is the type of system (3-phase (3p), 6-phase LV (6l), or 6-phase HV (6h)), and Top is the topology (DSHB, DSFB, SSHB, SSFB, or SDFB).

## Paper III: An Overview of 3- and 6-phase Battery Integrated Modular Multilevel Converters

by Arvind Balachandran, Tomas Jonsson, and Lars Eriksson. Submitted to *SAE International Journal of Electrified Vehicles*.

The potential benefit of introducing 6-phase BI-MMCs into hybrid- and battery-electric vehicles are investigated. The investigation considers a conventional 3-phase 2-level SiC MOSFET-based voltage source inverter as the reference case. It is compared alongside five different BI-MMC topologies for three main system configurations, namely 3-phase (presented in Paper I), 6-phase low voltage, and 6-phase high voltage systems for a 400 kW 40-ton commercial vehicle. Furthermore, the effect of the number of cascaded cells per submodule for all BI-MMC topologies on the number of submodules, battery losses, capacitor losses, and semiconductor losses is presented.

Traction, DC charging, electric roads, active submodule balancing, and parallel auxiliary power capabilities of all the BI-MMC topologies and systems are presented. A performance matrix of all BI-MMCs with their operating capabilities is developed. The performance matrix is the total number of submodules vs. the total system efficiency for all BI-MMC topologies and systems. The performance matrix is intended to aid an automotive designer to perform a cost-benefit comparative assessment of all the BI-MMC topologies for a desired operating mode.



The evaluation of the three different systems shows that the 3-phase system has the highest losses, and the 6-phase HV system has the least losses for a given topology or the number of cascaded cells per submodule. However, the 3-phase system has the least cost, while the 6-phase HV system has the most. Most of the full-bridge SM-based BI-MMC topologies have higher efficiency than the conventional 2-level inverter with a considerable increase in cost.

## Paper IV: DC Charging Capabilities of Battery-Integrated Modular Multilevel Converters Designed Based on a Maximum Tractive-Power

by Arvind Balachandran, Tomas Jonsson, and Lars Eriksson. Submitted to *MDPI journal Electricity, Special Issue: Modular Battery Systems and Advanced Energy Storage Solutions*.

The battery pack is connected directly to a DC charger in a conventional powertrain. However, the battery and the inverter are integrated in a BI-MMC. The derivation of the maximum DC charging power of five 3-phase BI-MMCs designed considering the same submodule semiconductor losses as for a maximum tractive power of 400 kW is presented.

A comparative assessment of five 3-phase BI-MMCs with 1, 6, and 12 cascaded cells per submodule, considering two different design criteria either based on the maximum motor voltage or maximum MCS DC charger voltage is presented. The assessment includes the maximum DC charging power, voltage, and current, the total number of submodules, submodule losses, total semiconductor losses, and submodule temperature at maximum charging power. The two different design criteria for the total number of submodules are: first, the output AC voltage determines the total number of submodules as presented in Paper I (CDC-T). Second, the total number of submodules in Paper I is changed such that the maximum MCS DC charger voltage defines the total number of submodules (CDC-C).

Almost all BI-MMC topologies with CDC-C have significantly higher charging power than topologies with CDC-T at the cost of increased total losses. As

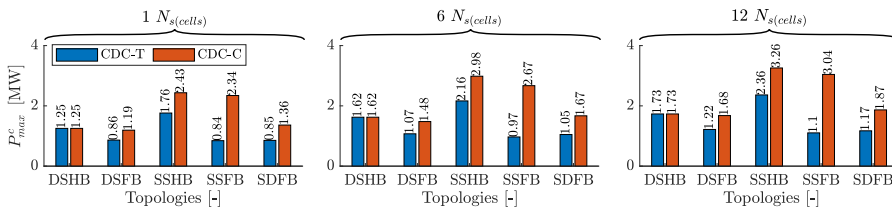


**Figure 5:** The maximum DC charging power considering the two different DC-charging scenarios, (CDC-T) and (CDC-C), for all topologies with 1, 6, and 12  $N_{s(cells)}$  presented in Paper IV.

the number of cascaded cells ( $N_{s(cells)}$ ) increases, the maximum DC charging power also increases. The maximum DC charging power is highest for the single-star half-bridge BI-MMC topology with 12  $N_{s(cells)}$  at about 3.3 MW, and is lowest for single-star full-bridge topology with 1  $N_{s(cells)}$  at about 800 kW.

## 3.2 Future Work

The topology evaluations presented in Papers I to IV considered only a single operating point in the drive cycle. Therefore, developing a complete efficiency map for BI-MMC topologies for the traction motor's full speed and torque ranges is an intended future research activity.

Papers I to III considered a phase-shifted carrier-based modulation for simplicity. A possible future research direction is investigating the impact of different modulation schemes, such as nearest-level modulation, selective harmonic elimination, direct torque control, etc., on the battery current and the output voltage. Another future research prospect is to quantify the benefits of having a multi-level output voltage on the traction motor, particularly on the motor design and reliability.

The arm inductor in a conventional MMC is designed to suppress the circulating current and limit the fault current rise rate. Since the circulating currents in BI-MMCs and conventional MMCs are different, future research activity is to develop a design principle for the arm inductor.

Paper IV presents the continuous DC charging capabilities of BI-MMCs assuming the same submodule semiconductor losses during traction at maximum tractive power. Several pieces of research indicate an improvement in battery life with pulsed charging current [76, 77]. Therefore, future research will extend the work in Paper IV to pulsed charging.

Paper IV considered individual BI-MMC submodules as buck converters, limiting the maximum DC charger voltage. A higher DC charging voltage is achieved by operating the submodules as buck-boost converters, which also is a proposed future research direction.

---

## References

- [1] F. Nistor and C. C. Popa. The role of transport in economic development. 2014.
- [2] Trucks - european automobile manufacturers association. URL [https://acea.auto/files/factsheet\\_trucks.pdf](https://acea.auto/files/factsheet_trucks.pdf).
- [3] Federal vehicle standards, Mar 2022. URL <https://www.c2es.org/content/regulating-transportation-sector-carbon-emissions/>.
- [4] C. J. Bonfils, B. D. Santer, J. C. Fyfe, K. Marvel, T. J. Phillips, and S. R. Zimmerman. Human influence on joint changes in temperature, rainfall and continental aridity. *Nature Climate Change*, 10(8):726–731, 2020.
- [5] Ö. Andersson and P. Börjesson. The greenhouse gas emissions of an electrified vehicle combined with renewable fuels: Life cycle assessment and policy implications. *Applied Energy*, 289:116621, 2021.
- [6] Z. Hausfather and P. Friedlingstein. Analysis: Global co2 emissions from fossil fuels hit record high in 2022. URL <https://www.carbonbrief.org/analysis-global-co2-emissions-from-fossil-fuels-hit-record-high-in-2022/>.
- [7] T. Boden, G. Marland, and R. Andres. Global, regional, and national fossil-fuel co2 emissions. carbon dioxide information analysis center, oak ridge national laboratory. *US Department of Energy, Oak Ridge, Tenn., USA 2009. doi 10.3334/CDIAC*, 1, 2017.
- [8] I. C. Change et al. Mitigation of climate change. *Contribution of working group III to the fifth assessment report of the intergovernmental panel on climate change*, 1454:147, 2014.
- [9] NOAA national centers for environmental information, 2022. URL <https://www.ncei.noaa.gov/access/monitoring/monthly-report/global/202209>.
- [10] E. Commission. Communication from the commission to the european parliament, the council, the european economic and social committee and the committee of the regions youth opportunities initiative. 2011.
- [11] S. Manzetti and F. Mariasiu. Electric vehicle battery technologies: From present state to future systems. *Renewable and Sustainable Energy Reviews*, 51:1004–1012, 2015.

- [12] D. Pevec, J. Babic, A. Carvalho, Y. Ghiassi-Farrokhfal, W. Ketter, and V. Podobnik. Electric vehicle range anxiety: An obstacle for the personal transportation (r) evolution? In *2019 4th international conference on smart and sustainable technologies (splitech)*, pages 1–8. IEEE, 2019.
- [13] P.-L. Ragon and F. Rodríguez. Co<sub>2</sub> emissions from trucks in the eu: An analysis of the heavy-duty co<sub>2</sub> standards baseline data. Technical report, 2021.
- [14] J. Neubauer and E. Wood. The impact of range anxiety and home, workplace, and public charging infrastructure on simulated battery electric vehicle lifetime utility. *Journal of power sources*, 257:12–20, 2014.
- [15] D. Pevec, J. Babic, A. Carvalho, Y. Ghiassi-Farrokhfal, W. Ketter, and V. Podobnik. A survey-based assessment of how existing and potential electric vehicle owners perceive range anxiety. *Journal of Cleaner Production*, 276:122779, 2020.
- [16] Vehicle mileage for swedish-registered vehicles. URL <https://www.trafa.se/en/road-traffic/driving-distances-with-swedish-registered-vehicles/>.
- [17] K. W. Beard. *Linden's handbook of batteries*. McGraw-Hill Education, 2019.
- [18] F. Sund and G. Erbing. Battery digital twin: Modeling and characterization of a lithium-ion battery, 2021.
- [19] B. Scrosati. History of lithium batteries. *Journal of solid state electrochemistry*, 15(7):1623–1630, 2011.
- [20] C. Drucker. Die stromliefernden vorgänge des leclanché-elements. *Zeitschrift für Physikalische Chemie*, 1931(Supplement):912–918, 1931.
- [21] M. Winter, B. Barnett, and K. Xu. Before li ion batteries. *Chemical reviews*, 118(23):11433–11456, 2018.
- [22] J. T. Warner. *The handbook of lithium-ion battery pack design: chemistry, components, types and terminology*. Elsevier, 2015.
- [23] L. Guzzella, A. Sciarretta, et al. *Vehicle propulsion systems*, volume 1. Springer, 2007.
- [24] G. L. Plett. *Battery management systems, Volume II: Equivalent-circuit methods*. Artech House, 2015.
- [25] H. Berg. *Batteries for electric vehicles: materials and electrochemistry*. Cambridge university press, 2015.
- [26] C. S. Goli, S. Essakiappan, P. Sahu, M. Manjrekar, and N. Shah. Review of recent trends in design of traction inverters for electric vehicle applications. In *2021 IEEE 12th International Symposium on Power Electronics for Distributed Generation Systems (PEDG)*, pages 1–6. IEEE, 2021.
- [27] D. Yoney. 7 electric cars with the biggest batteries, Jun 2018. URL <https://insideevs.com/features/336680/7-electric-cars-with-the-biggest-batteries/>.

- [28] M. O’Leary. Battery packs for heavy-duty electric vehicles, May 2022. URL <https://www.volvogroup.com/en/news-and-media/news/2022/may/battery-packs-for-electric-vehicles.html>.
- [29] S. F. Schuster, M. J. Brand, P. Berg, M. Gleissenberger, and A. Jossen. Lithium-ion cell-to-cell variation during battery electric vehicle operation. *Journal of Power Sources*, 297:242–251, 2015.
- [30] J. Garche and K. Brandt. *Electrochemical Power Sources: Fundamentals, Systems, and Applications: Li-Battery Safety*. Elsevier, 2018.
- [31] W. Han, T. Wik, A. Kersten, G. Dong, and C. Zou. Next-generation battery management systems: Dynamic reconfiguration. *IEEE Industrial Electronics Magazine*, 14(4):20–31, 2020.
- [32] L. He, L. Kong, S. Lin, S. Ying, Y. Gu, T. He, and C. Liu. Reconfiguration-assisted charging in large-scale lithium-ion battery systems. In *2014 ACM/IEEE International Conference on Cyber-Physical Systems (ICCPS)*, pages 60–71. IEEE, 2014.
- [33] N. Bouchhima, M. Schnierle, S. Schulte, and K. P. Birke. Active model-based balancing strategy for self-reconfigurable batteries. *Journal of Power Sources*, 322: 129–137, 2016.
- [34] N. Lin and S. Ci. Toward dynamic programming-based management in reconfigurable battery packs. In *2017 IEEE Applied Power Electronics Conference and Exposition (APEC)*, pages 2136–2140. IEEE, 2017.
- [35] F. Altaf. *On Modeling and Optimal Control of Modular Batteries*. PhD thesis, Ph. D. dissertation, Chalmers University of Technology, 2016.
- [36] T. Kim, W. Qiao, and L. Qu. Series-connected self-reconfigurable multicell battery. In *2011 Twenty-Sixth Annual IEEE Applied Power Electronics Conference and Exposition (APEC)*, pages 1382–1387. IEEE, 2011.
- [37] T. Kim, W. Qiao, and L. Qu. A series-connected self-reconfigurable multicell battery capable of safe and effective charging/discharging and balancing operations. In *2012 Twenty-Seventh Annual IEEE Applied Power Electronics Conference and Exposition (APEC)*, pages 2259–2264. IEEE, 2012.
- [38] M. Momayyezani, B. Hredzak, and V. G. Agelidis. Integrated reconfigurable converter topology for high-voltage battery systems. *IEEE Transactions on Power Electronics*, 31(3):1968–1979, 2015.
- [39] T. Morstyn, M. Momayyezani, B. Hredzak, and V. G. Agelidis. Distributed control for state-of-charge balancing between the modules of a reconfigurable battery energy storage system. *IEEE Transactions on Power Electronics*, 31(11):7986–7995, 2015.
- [40] Y. Kim, S. Park, Y. Wang, Q. Xie, N. Chang, M. Poncino, and M. Pedram. Balanced reconfiguration of storage banks in a hybrid electrical energy storage system. In *2011 IEEE/ACM International Conference on Computer-Aided Design (ICCAD)*, pages 624–631. IEEE, 2011.

- [41] H. Visairo and P. Kumar. A reconfigurable battery pack for improving power conversion efficiency in portable devices. In *2008 7th International Caribbean Conference on Devices, Circuits and Systems*, pages 1–6. IEEE, 2008.
- [42] S. Steinhorst, Z. Shao, S. Chakraborty, M. Kauer, S. Li, M. Lukasiewicz, S. Narayanaswamy, M. U. Rafique, and Q. Wang. Distributed reconfigurable battery system management architectures. In *2016 21st Asia and South Pacific Design Automation Conference (ASP-DAC)*, pages 429–434. IEEE, 2016.
- [43] S. Ci, J. Zhang, H. Sharif, and M. Alahmad. Dynamic reconfigurable multi-cell battery: A novel approach to improve battery performance. In *2012 Twenty-Seventh Annual IEEE Applied Power Electronics Conference and Exposition (APEC)*, pages 439–442. IEEE, 2012.
- [44] L. He, E. Kim, and K. G. Shin. A case study on improving capacity delivery of battery packs via reconfiguration. *ACM Transactions on Cyber-Physical Systems*, 1(2):1–23, 2017.
- [45] V. Sukumar, M. Alahmad, K. Buck, H. Hess, H. Li, D. Cox, F. N. Zghoul, J. Jackson, S. Terry, B. Blalock, et al. Switch array system for thin film lithium micro-batteries. *Journal of power sources*, 136(2):401–407, 2004.
- [46] H. Kim and K. G. Shin. On dynamic reconfiguration of a large-scale battery system. In *2009 15th IEEE Real-Time and Embedded Technology and Applications Symposium*, pages 87–96. IEEE, 2009.
- [47] D. G. Holmes and T. A. Lipo. *Pulse width modulation for power converters: principles and practice*, volume 18. John Wiley & Sons, 2003.
- [48] E. A. Grunditz. *Design and assessment of battery electric vehicle powertrain, with respect to performance, energy consumption and electric motor thermal capability*. Chalmers Tekniska Hogskola (Sweden), 2016.
- [49] K. Sharifabadi, L. Harnefors, H.-P. Nee, S. Norrga, and R. Teodorescu. *Design, control, and application of modular multilevel converters for HVDC transmission systems*. John Wiley & Sons, 2016.
- [50] A. Lesnicar and R. Marquardt. An innovative modular multilevel converter topology suitable for a wide power range. In *2003 IEEE Bologna Power Tech Conference Proceedings*, volume 3, pages 6–pp. IEEE, 2003.
- [51] N. Mohan. *Power electronics: a first course*. Wiley, 2011.
- [52] I. Trintis, S. Munk-Nielsen, and R. Teodorescu. A new modular multilevel converter with integrated energy storage. In *IECON 2011-37th Annual Conference of the IEEE Industrial Electronics Society*, pages 1075–1080. IEEE, 2011.
- [53] J. I. Y. Ota, T. Sato, and H. Akagi. Enhancement of performance, availability, and flexibility of a battery energy storage system based on a modular multilevel cascaded converter (mmcc-ssbc). *IEEE Transactions on Power Electronics*, 31(4): 2791–2799, 2015.

- [54] A. Lachichi. On modular multilevel converters-based batteries energy storage systems. In *2015 IEEE 11th International Conference on Power Electronics and Drive Systems*, pages 908–912. IEEE, 2015.
- [55] G. Brando, A. Dannier, I. Spina, and P. Tricoli. Integrated bms-mmc balancing technique highlighted by a novel space-vector based approach for bevs application. *Energies*, 10(10):1628, 2017.
- [56] Z. Wang, H. Lin, Y. Ma, X. Wang, T. Wang, and Z. Ze. Analysis and control strategy of modular multilevel converter with integrated battery energy storages system based on voltage source mode. In *2018 20th European Conference on Power Electronics and Applications (EPE'18 ECCE Europe)*, pages P–1. IEEE, 2018.
- [57] L. Baruschka and A. Mertens. Comparison of cascaded H-bridge and modular multilevel converters for BESS application. In *2011 IEEE Energy Conversion Congress and Exposition*, pages 909–916. IEEE, 2011.
- [58] M. Quraan, T. Yeo, and P. Tricoli. Design and control of modular multilevel converters for battery electric vehicles. *IEEE Transactions on Power Electronics*, 31(1):507–517, 2015.
- [59] M. Tsirinomeny and A. Rufer. Configurable modular multilevel converter (cmmc) for flexible ev. In *2015 17th European Conference on Power Electronics and Applications (EPE'15 ECCE-Europe)*, pages 1–10. IEEE, 2015.
- [60] Y. Ma, H. Lin, X. Wang, Z. Wang, and Z. Ze. Analysis of battery fault tolerance in modular multilevel converter with integrated battery energy storage system. In *2018 20th European Conference on Power Electronics and Applications (EPE'18 ECCE Europe)*, pages P–1. IEEE, 2018.
- [61] C. Gan, Q. Sun, J. Wu, W. Kong, C. Shi, and Y. Hu. Mmc-based srm drives with decentralized battery energy storage system for hybrid electric vehicles. *IEEE transactions on power electronics*, 34(3):2608–2621, 2018.
- [62] R. Hariri, F. Sebaaly, and H. Y. Kanaan. A review on modular multilevel converters in electric vehicles. In *IECON 2020 The 46th Annual Conference of the IEEE Industrial Electronics Society*, pages 4987–1993. IEEE, 2020.
- [63] C. Korte, E. Specht, M. Hiller, and S. Goetz. Efficiency evaluation of mmspc/chb topologies for automotive applications. In *2017 IEEE 12th International Conference on Power Electronics and Drive Systems (PEDS)*, pages 324–330. IEEE, 2017.
- [64] N. Sorokina, J. Estaller, A. Kersten, J. Buberger, M. Kuder, T. Thiringer, R. Ecklerle, and T. Weyh. Inverter and battery drive cycle efficiency comparisons of multilevel and two-level traction inverters for battery electric vehicles. In *2021 IEEE International Conference on Environment and Electrical Engineering and 2021 IEEE Industrial and Commercial Power Systems Europe (EEEIC/I&CPS Europe)*, pages 1–8. IEEE, 2021.

- [65] F. Chang, O. Ilina, M. Lienkamp, and L. Voss. Improving the overall efficiency of automotive inverters using a multilevel converter composed of low voltage si mosfet s. *IEEE Transactions on Power Electronics*, 34(4):3586–3602, 2018.
- [66] F. Helling, M. Kuder, A. Singer, S. Schmid, and T. Weyh. Low voltage power supply in modular multilevel converter based split battery systems for electrical vehicles. In *2018 20th European Conference on Power Electronics and Applications (EPE'18 ECCE Europe)*, pages P–1. IEEE, 2018.
- [67] A. Kersten, M. Kuder, E. Grunditz, Z. Geng, E. Wikner, T. Thiringer, T. Weyh, and R. Eckerle. Inverter and battery drive cycle efficiency comparisons of chb and mmstp traction inverters for electric vehicles. In *2019 21st European Conference on Power Electronics and Applications (EPE'19 ECCE Europe)*, pages P–1. IEEE, 2019.
- [68] F. Helling, S. Götz, and T. Weyh. A battery modular multilevel management system (bm3) for electric vehicles and stationary energy storage systems. In *2014 16th European Conference on Power Electronics and Applications*, pages 1–10. IEEE, 2014.
- [69] O. Theliander, A. Kersten, M. Kuder, W. Han, E. A. Grunditz, and T. Thiringer. Battery modeling and parameter extraction for drive cycle loss evaluation of a modular battery system for vehicles based on a cascaded h-bridge multilevel inverter. *IEEE Transactions on Industry Applications*, 56(6):6968–6977, 2020.
- [70] F. Chang, O. Ilina, O. Hegazi, L. Voss, and M. Lienkamp. Adopting mosfet multilevel inverters to improve the partial load efficiency of electric vehicles. In *2017 19th European Conference on Power Electronics and Applications (EPE'17 ECCE Europe)*, pages P–1. IEEE, 2017.
- [71] N. Sorokina, J. Estaller, M. Kuder, W. Grupp, A. Lesnicar, R. Eckerle, and T. Weyh. Efficiency investigation of a battery modular multilevel management converter system. In *PCIM Europe 2022; International Exhibition and Conference for Power Electronics, Intelligent Motion, Renewable Energy and Energy Management*, pages 1–8. VDE, 2022.
- [72] S. D’Arco, L. Piegari, M. Quraan, and P. Tricoli. Battery charging for electric vehicles with modular multilevel traction drives. 2014.
- [73] T. Martel and A. Rufer. Electric vehicle driving and fast charging system based on configurable modular multilevel converter (cmmc). In *2013 15th European Conference on Power Electronics and Applications (EPE)*, pages 1–10. IEEE, 2013.
- [74] J. Buberger, J. Estaller, W. Grupp, F. Schwitzgebel, A. Wiedenmann, A. Mashayekh, M. Kuder, R. Eckerle, and T. Weyh. Ac and dc charging for electric vehicles with a battery modular multilevel management (bm3) converter system. In *PCIM Europe 2022; International Exhibition and Conference for Power Electronics, Intelligent Motion, Renewable Energy and Energy Management*, pages 1–8. VDE, 2022.



- [75] J. Buberger, A. Kersten, M. Kuder, A. Singer, A. Mashayekh, J. Estaller, T. Thiringer, R. Eckerle, and T. Weyh. Charging strategy for battery electric vehicles with a battery modular multilevel management (bm3) converter system using a pr controller. In *2021 23rd European Conference on Power Electronics and Applications (EPE'21 ECCE Europe)*, pages P-1. IEEE, 2021.
- [76] E. Goldammer, M. Gentejohann, M. Schlüter, D. Weber, W. Wondrak, S. Dieckhoff, C. Gühmann, and J. Kowal. The impact of an overlaid ripple current on battery aging: The development of the sicwell dataset. *Batteries*, 8(2):11, 2022.
- [77] X. Huang, Y. Li, A. B. Acharya, X. Sui, J. Meng, R. Teodorescu, and D.-I. Stroe. A review of pulsed current technique for lithium-ion batteries. *Energies*, 13(10):2458, 2020.



# PAPERS

# Papers

The papers associated with this thesis have been removed for copyright reasons. For more details about these see:

<https://doi.org/10.3384/9789180750172>

Licentiate Dissertations  
Division of Vehicular Systems  
Department of Electrical Engineering  
Linköping University

- No. 1 Magnus Pettersson, *Driveline Modeling and Principles for Speed Control and Gear-Shift Control*, 1996.
- No. 2 Lars Eriksson, *Closed-Loop Spark-Advance Control using the Spark Plug as Ion Probe*, 1997.
- No. 3 Mattias Nyberg, *Model Based Diagnosis with Application to Automotive Engines*, 1997.
- No. 4 Erik Frisk, *Residual Generation for Fault Diagnosis: Nominal and Robust Design*, 1998.
- No. 5 Tony Sandberg, *Heavy Truck Modeling for Fuel Consumption: Simulations and Measurements*, 2001.
- No. 6 Per Andersson, *Intake Air Dynamics on a Turbocharged SI-Engine with Wastegate*, 2002.
- No. 7 Ingemar Andersson, *Cylinder Pressure and Ionization Current Modeling for Spark Ignited Engines*, 2002.
- No. 8 Mattias Krysanter, *Design and Analysis of Diagnostic Systems Utilizing Structural Methods*, 2003.
- No. 9 Marcus Klein, *A specific heat ratio model and compression ratio estimation*, 2004.
- No. 10 Gunnar Cedersund, *System Identification of Nonlinear Thermochemical Systems with Dynamical Instabilities*, 2004.
- No. 11 Jonas Biteus, *System Identification of Nonlinear Thermochemical Systems with Dynamical Instabilities*, 2005.
- No. 12 Anders Fröberg, *Extending the Inverse Vehicle Propulsion Simulation Concept-To Improve Simulation Performance*, 2005.
- No. 13 Johan Wahlström, *Control of EGR and VGT for emission control and pumping work minimization in diesel engines*, 2006.
- No. 14 Erik Hellström, *Look-ahead Control of Heavy Trucks utilizing Road Topography*, 2007.
- No. 15 Erik Höckerdal, *Observer Design and Model Augmentation for Bias Compensation with Engine Applications*, 2008.
- No. 16 Maria Ivarsson, *Fuel Optimal Powertrain Control for Heavy Trucks Utilizing Look Ahead*, 2009.

- No. 17** Carl Svärd, *Residual Generation Methods for Fault Diagnosis with Automotive Applications*, 2009.
- No. 18** Oskar Leufvén, *Compressor Modeling for Control of Automotive Two Stage Turbochargers*, 2010.
- No. 19** Christofer Sundström, *Vehicle Level Diagnosis for Hybrid Powertrain*, 2011.
- No. 20** Emil Larsson, *Diagnosis and Supervision of Industrial Gas Turbines*, 2012.
- No. 22** Tomas Nilsson, *Optimal Engine Operation in a Multi-Mode CVT Wheel Loader*, 2012.
- No. 23** Daniel Eriksson, *Diagnosability analysis and FDI system design for uncertain systems*, 2013.
- No. 24** Peter Nyberg, *Evaluation, Transformation, and Extraction of Driving Cycles and Vehicle Operations*, 2013.
- No. 25** Kristoffer Lundahl, *Modeling and Optimization for Critical Vehicle Maneuvers*, 2013.
- No. 26** Andreas Myklebust, *Modeling and Estimation for Dry Clutch Control*, 2013.
- No. 27** Neda Nickmehr, *System Identification of an Engine-load Setup Using Grey-box Model*, 2014.
- No. 28** Sergii Voronov, *Data-driven lead-acid battery lifetime prognostics*, 2017.
- No. 29** Victor Fors, *Optimal Braking Patterns and Forces in Autonomous Safety-Critical Maneuvers*, 2018.
- No. 30** Jörgen Albrektsson, *Optimisation of Off-Road Transport Missions*, 2018.
- No. 31** Pavel Anistratov, *Computation of Autonomous Safety Maneuvers Using Segmentation and Optimization*, 2019.
- No. 32** Erik Jakobsson, *Data-driven Condition Monitoring in Mining Vehicles*, 2019.
- No. 33** Arvind Balachandran, *Battery Integrated Modular Multilevel Converter Topologies for Automotive Applications*, 2023.

# FACULTY OF SCIENCE AND ENGINEERING

Linköping Studies in Science and Technology, Licentiate Thesis No. 1952, 2023  
Department of Electrical Engineering

Linköping University  
SE-581 83 Linköping, Sweden

[www.liu.se](http://www.liu.se)

```
1 uout = zeros(1, length(tsim)); % initialization
2 idc_mtx = struct; % the dc current vector initialization
3 cout = zeros(1, length(tsim)); % the dc current vector initialization
4
5 switch modulation_scheme(1)
6     case 'pspwm1'
7         ref = M*sin(2*pi*f.*tsim); % reference vector
8     case 'pspwm3'
9         ref = M*(sin(2*pi*f.*tsim) - sin(2*3*pi*f.*tsim)/6); % reference vector
10    case 'psvpwm'
11        ref = M*(sin(2*pi*f.*tsim) - sawtooth(3*(2*pi*f.*tsim)-pi/2,0.5)/6); % reference vector
12    otherwise
13        error('Select a modulation scheme!');
14
15 end
16
17 %% carrier, output voltage and dc currents calculations
18 fprintf('Started output voltage and dc currents calculations with %s modulation scheme\n', modulation_scheme);
19 tstart = tic;
20
21 for ii = 1:length(NoofPhases)
22     for jj = 1:length(Topologies)
23         for kk = 1:length(NoofCells)
24             Us_temp = Us(jj,kk,ii); % input voltage of SM
25             iarm_temp = iarm_pk(jj,kk,ii)*sin(2*pi*f.*tsim - acos(cosphi)); % arm current
26             if Topologies(jj) == 1 || Topologies(jj) == 3
27                 nlvs = linspace(0,2*pi,ceil(NoofSM.arm(jj,kk,ii)));
28             else
29                 nlvs = linspace(0,pi,ceil(NoofSM.arm(jj,kk,ii)));
30             end
31             carr = sawtooth(2*pi*fsw_mtx(jj,kk,ii).*tsim + nlvs',0.5); % carrier
32             % MOSFET switching functions
33             s1 = single(ref>carr); s2 = single(ref<carr);
34             s3 = single(-ref>carr); s4 = single(-ref<carr);
35             is1 = single(iarm_temp.*s1);
36             idc_mtx(jj,kk,ii).is2 = single(-iarm_temp.*s2);
37             is3 = single(-iarm_temp.*s3);
38             idc_mtx(jj,kk,ii).is4 = single(iarm_temp.*s4);
39             if Topologies(jj) == 1 || Topologies(jj) == 3
40                 usm_temp_u = Us_temp*s1;
41                 usm_temp_f = Us_temp*s3;
42                 switch Topologies(jj)
43                     case 1
44                         uout(jj,kk,ii,:) = single(sum((usm_temp_u - usm_temp_f),1));
45                     case 3
46                         uout(jj,kk,ii,:) = single(sum((usm_temp_u),1));
47                 end
48                 idc_mtx(jj,kk,ii).idc = is1;
49             else
50                 usm_temp = Us_temp.*(s1 - s3);
51                 uout(jj,kk,ii,:) = single(sum((usm_temp),1));
52                 idc_mtx(jj,kk,ii).idc = is1 + is3;
53             end
54         end
55     end
56 end
```